

One of us (HM) is grateful to NTNF and NAVF for the financial support. Thanks are due also to Dr T. Norby for help with the specimen preparation.

References

- ARLINGHAUS, F. J. (1974). *J. Phys. Chem. Solids*, **35**, 931–935.
 BAUR, W. & KHAN, A. (1971). *Acta Cryst.* **B27**, 2133–2139.
 BURSILL, L. A., PING, A., SMITH, D. J. & SHANNON, M. D. (1981). *Philos. Mag.* **A45**, 771–789.
 CROMER, D. T. & MANN, J. B. (1968). *Acta Cryst.* **A24**, 321–324.
 DOYLE, P. A. & TURNER, P. S. (1968). *Acta Cryst.* **A24**, 390–397.
 GJØNNES, J. & HØIER, R. (1971). *Acta Cryst.* **A27**, 313–316.
 HIRSCH, P. B., HOWIE, A., NICHOLSON, R. B., PASHLEY, D. W. & WHELAN, M. J. (1965). *Electron Microscopy of Thin Crystals*. London: Butterworth.
 HØIER, R. (1969). *Acta Cryst.* **A25**, 516–518.
 MATSUHATA, H. & GJØNNES, J. (1994). *Acta Cryst.* **A50**, 107–115.
 RESTORI, R., SCHWARZENBACH, D. & SCHNEIDER, J. R. (1987). *Acta Cryst.* **B43**, 251–257.
 SHANNON M. D. & STEEDS J. W. (1977) *Philos. Mag.* **A36**, 279–307.
 TOKONAMI, M. (1965). *Acta Cryst.* **19**, 486.
 WATANABE, D., UYEDA, R. & FUKUHARA, A. (1969). *Acta Cryst.* **A25**, 138–140.

SHORT COMMUNICATIONS

Acta Cryst. (1994). **A50**, 123

Multipole analysis of X-ray diffraction data on BeO. Erratum. By GENEVIÈVE VIDAL-VALAT and JEAN-PIERRE VIDAL, *Groupe de Dynamique des Phases Condensées (UA CNRS 233), Université Montpellier II, 34095 Montpellier CEDEX 5, France*, and KAARLE KURKI-SUONIO and RIITTA KURKI-SUONIO, *Department of Physics, University of Helsinki, Siltavuorenpenger 20D, PO Box 9, SF-00014 Helsinki, Finland*

(Received 25 October 1993)

Abstract

A misprint in the paper by Vidal-Valat, Vidal, Kurki-Suonio & Kurki-Suonio [*Acta Cryst.* (1987), **A43**, 540–550] is corrected.

On Fig. 1, the value 2.7823 Å should read 2.7283 Å.

Professor E.-F. Bertaut is thanked for bringing our attention to this misprint.

Acta Cryst. (1994). **A50**, 123–126

Concerning the components contributing to Bragg reflection profile shapes in synchrotron-radiation studies of small single crystals. By A. MCL. MATHIESON, *Chemistry Department, La Trobe University, Bundoora, Victoria 3083, Australia*, and *Division of Materials Science and Technology, CSIRO, Private Bag 33, Rosebank MDC, Victoria 3169, Australia*

(Received 22 July 1993; accepted 8 September 1993)

Abstract

Certain basic matters in a recent synchrotron-radiation study [Rossmannith (1993). *Acta Cryst.* **A49**, 80–91] and an allied study which developed a new peak-width formula [Rossmannith (1992). *Acta Cryst.* **A48**, 596–610] are questioned. These matters concern the mode of combination of certain components which determine the one-dimensional profile shape of Bragg reflections and the functional form of the wavelength dispersion dependence on the Bragg angle of the sample crystal and that of a monochromator crystal where the respective crystal axes are parallel.

1. Introduction

A recent synchrotron-radiation study by Rossmannith (1993; hereafter *R93*) dealt with the various individual components which combine to determine the one-dimensional profile shape of Bragg reflections from a small specimen crystal, *c*, as the Bragg angle of the crystal, θ_c , changes. The synchrotron

radiation convergent on *c* comes from a monochromator crystal, *M*, and corresponds to a wavelength band, $\Delta\lambda$. In an earlier publication, Rossmannith (1992; hereafter *R92*) introduced an additional component, called the 'particle-size effect' in *R93*, and denoted by ε . By incorporating this component with the wavelength-dispersion component, a new peak-width formula was derived in *R92* (non-monochromator case) and in *R93* (monochromator case). The modes of combination of components in *R92* and *R93* and the derivation of the functional form of the wavelength dispersion in *R93* differ significantly from those associated with earlier published works and, therefore, they warrant comment.

2. Identification of the components in diffraction space and their mode(s) of combination (non-monochromator case)

To identify the various components and their contribution to the shapes of one-dimensional profiles, there is considerable advantage in approaching the situation from a two-dimensional

viewpoint, such as $\Delta\omega, \Delta 2\theta$ space (Mathieson, 1982) since it effectively 'deconstructs' the one-dimensional distribution. $\Delta\omega_c$ is the differential angular displacement of c (and hence of the reciprocal lattice about the origin) in respect of a given reflection and $\Delta 2\theta_c$ is the corresponding differential angular displacement of a beam diffracted from the specimen crystal. (To refer to $\Delta\theta_c$ when one means $\Delta\omega_c$ is misleading.) The one-dimensional profile, $I(\Delta\omega_c)$, corresponds to an integration across $\Delta 2\theta_c$ (associated with the 'wide' aperture of the detector).

For a given reflection, each component distribution has a well defined locus in $\Delta\omega, \Delta 2\theta$ space, Fig. 1(a). One can therefore identify the main individual components, namely, the specimen crystal mosaic distribution, μ (terminology as in Mathieson, 1982; $\mu = \eta$ in R92, R93) (locus parallel to the $\Delta\omega$ axis), the source-emissivity distribution, σ (locus at 45° to the $\Delta\omega$ and $\Delta 2\theta$ axes), and the wavelength distribution, λ [locus at $\arctan(1/2)$ to the $\Delta 2\theta$ axis], all in respect of the ω -scan mode. If the loci of two components are parallel, then they will be combined by convolution. If the loci are non-parallel, they have to be combined either by cross-multiplication or by convolution (see Mathieson, 1984; Mathieson & Stevenson, 1993). When the components in $\Delta\omega, \Delta 2\theta$ space are projected onto one dimension, $\Delta\omega$ (say), their distributions all have to be combined by convolution, see *Discussion* in Mathieson & Stevenson (1993). This corresponds to the basic approach for synthesizing (modelling) one-dimensional profiles presented by Alexander & Smith (1962) (*cf.* Stokes, 1948) and utilized subsequently by many authors over the last three decades, a

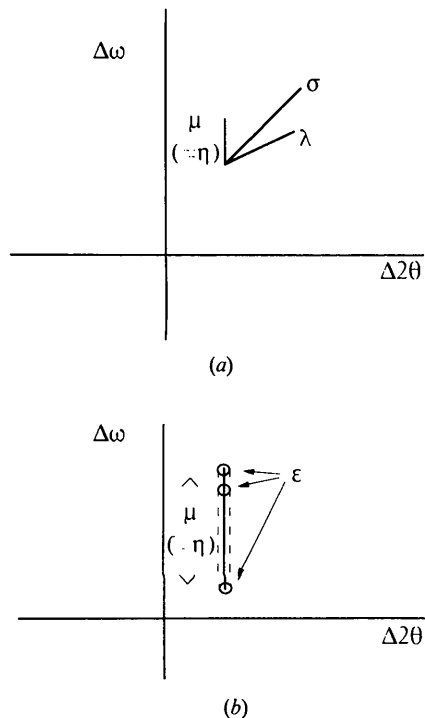


Fig. 1. Diagram in $\Delta\omega, \Delta 2\theta$ space, with terminology as in Mathieson (1982), of (a) the loci of the mosaic distribution, $\mu (= \eta$ in R92, R93), the source-emissivity distribution, σ , and the wavelength distribution, λ . (b) Superposition of the particle-size effect, ϵ , on the points of the mosaic distribution, $\mu (= \eta)$, to indicate their combined distribution (dashed line) representing the inner morphology of the specimen crystal.

recent example being the work of Destro & Marsh (1993). For the non-monochromator case, the dependence of the wavelength-dispersion component, $|\Delta\omega_\lambda|$, versus $\tan\theta_c$ is shown in Fig. 2(a).

3. The distinction between scan range and profile width

In R92 (and R93), the widths of profile peaks are taken as full width at half-maximum (FWHM). The mode of combining the FWHM of the various components to determine the peak width, $\Delta\theta_h$, is specified as addition. Thus, p. 600 in R92 'The peak width $\Delta\theta_h$ is therefore given by the angle P_1OP_1' '. It is obvious from Fig. 3(d) that

$$\Delta\theta_h = \delta_2 + \delta - \delta_1 + \eta. \quad (6a)'$$

On p. 601, it is stated 'In Fig. 4, the peak width calculated with (6a) and (6b) respectively are compared with experimental values. The full width at half-maximum (FWHM) values for the Cu $K\alpha_1$ component have been estimated...'. See also Fig. 4 and its caption.

In respect of these matters, there appears to be confusion in R92 (and R93) between the mode of combining components which is appropriate to establish the width of the rocking curve (scan range) and that which is appropriate to establish the width of the profile at some proportion of its peak maximum, usually half.

The scan range, $Sc(\Delta\omega)$, is determined by the outer limits (Lt) of the individual components and these are combined by

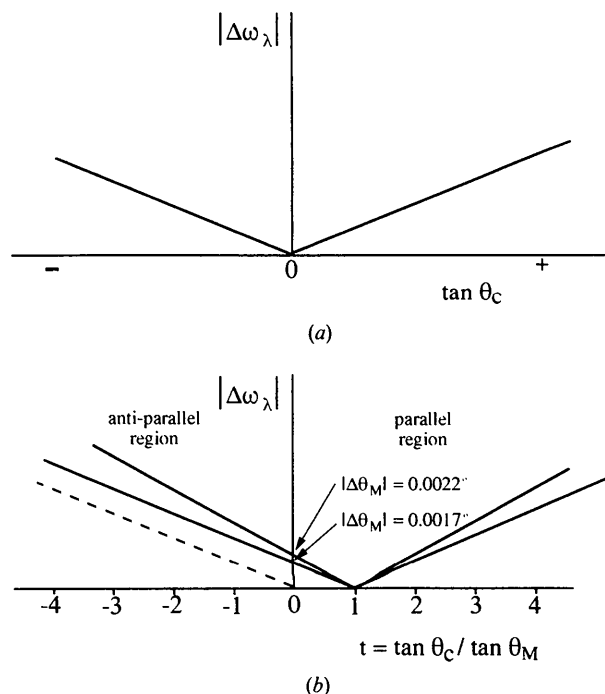


Fig. 2. Variation of the modulus of the angular contribution of the wavelength dispersion, $|\Delta\omega_\lambda|$, as the Bragg angle θ_c changes. (a) In the non-monochromator case, plotted against $\tan\theta_c$. (b) In the monochromator case, plotted against $t = \tan\theta_c / \tan\theta_M$. The full lines derive from Mathieson (1985a,b) and intersect the $|\Delta\omega_\lambda|$ axis at the respective values of $\Delta\theta_M$. Two possible values of $\Delta\theta_M$ are shown, for (i) 0.0017 and (ii) 0.0022° . The dashed line corresponds to the data presented in Fig. 5 of R93.

addition as in the following equation.

$$\begin{aligned} \text{Sc}(\Delta\omega) = & \text{Lt}[f_\lambda(\Delta\omega)] + \text{Lt}[f_\sigma(\Delta\omega)] + \text{Lt}[f_c(\Delta\omega)] \\ & + \text{Lt}[f_\eta(\Delta\omega)] + \text{Lt}[f_\varepsilon(\Delta\omega)], \end{aligned} \quad (A)$$

where the components are the wavelength (λ), source emissivity (σ), crystal size (c), mosaic spread (η) and the 'particle-size effect' (ε) introduced in *R92* and *R93*.

Relationship (A) is in accord with the (total) width of the rocking curve given by Arndt & Willis (1966), pp. 174, 267, and also in *International Tables for Crystallography* (1992).

The width at half-maximum (FWHM) of the profile, $I(\Delta\omega)$, depends upon the distributions, $f_x(\Delta\omega)$, of the various individual components and their mode of combination. The accepted mode of combination for the one-dimensional profile, $I(\Delta\omega)$, is by convolution as indicated in

$$I(\Delta\omega) = f_\lambda(\Delta\omega) * f_\sigma(\Delta\omega) * f_c(\Delta\omega) * f_\eta(\Delta\omega) * f_\varepsilon(\Delta\omega), \quad (B)$$

according to Alexander & Smith [1962; equations (1) and (2)]. If it were the case that every component was Gaussian in shape, then the FWHM of the derived distribution would correspond to the square root of the sum of the squares of the FWHM of the components.

An appropriate illustration of the considerable difference between the results derived from applying the two operations is by reference to the original example given by Alexander & Smith (1962). The angular limit widths at the base of the four distributions, given in Fig. 11 there, add up to 1.8° which, therefore, is the full scan range necessary to encompass the contributions of the four components, see Fig. 12. The FWHM of the distribution, $I(\Delta\omega)$, in Fig. 12 derived by convolution of the four distributions is 0.345° .

4. The component ε

In *R92* and *R93*, Rossmanith introduced the additional component, the 'particle-size effect' denoted by ε (*cf.* Wilson, 1949, p. 4). $\varepsilon = 1/r$ where r is the radius of an ideally perfect crystal (or of crystallites composing the macrocrystal). This component, ε , is one aspect of the inner morphology of the specimen crystal, namely the size of the crystallites. Another aspect is the angular (mosaic) distribution, η , of the crystallites. Obviously, the 'particle-size effect' applies in respect of all points of the mosaic distribution. If one accepts $I(\Delta\omega)$ as given in (B) above, there is no reason to differentiate the treatment of ε and η in respect of their combination with the other components. So, in the process of combining components, *cf.* Alexander & Smith [1962; equation (1)], these two components can be combined by convolution to provide a distribution which represents the overall inner morphology of the specimen, see Fig. 1(b), outer limit shown by the dashed line.

In *R92* and *R93* however, Rossmanith treats ε differently from η . ε is combined with the wavelength band to derive geometrical relationships given by equation (2b) in *R92* and equations (6b) and (6c) in *R93*, whereas η is combined additively in equation (5) in *R92* and equations (6a) and (7a) in *R93*.

Two points arise: (1) The reasons for following this procedure instead of the well established procedure expressed in (B) are not discussed by Rossmanith. (2) Neither of the combinative (essentially additive) procedures applied to ε or to η in *R92* and *R93* is appropriate to the derivation of FWHM. So comparison of the FWHM of profiles modelled on the Rossmanith procedure with FWHM of experimental profiles

is liable, at the very least, to lead to non-realistic physical parameters.*

5. Identification of the wavelength dispersion in $\Delta\omega, \Delta 2\theta$ space (monochromator case)

Where a monochromator, M , is involved and the axis of M is parallel to that of c , the wavelength dispersion of M and that of c interact (Mathieson 1985a,b; hereafter *M85a,b*). In $\Delta\omega, \Delta 2\theta$ space, the wavelength dispersion of M corresponds to a fixed vector $(-\Delta\theta_M, -\Delta\theta_M)$ [see equations (1) and (2) in *M85a*], which may also be given as $[(-\Delta\lambda/\lambda) \tan \theta_M, (-\Delta\lambda/\lambda) \tan \theta_M]$. The wavelength dispersion of c corresponds to a vector, origin at $(-\Delta\theta_M, -\Delta\theta_M)$, of length $(5)^{1/2}(\Delta\lambda/\lambda) \tan \theta_c$, with slope $\arctan(1/2)$ to the $\Delta 2\theta$ axis. The combination of these two results in a vector which, in the parallel region, rotates anticlockwise with increase in θ_c , being antiparallel to the $\Delta\omega$ axis when $\tan \theta_c / \tan \theta_M = (1/2)$ and parallel to the $\Delta 2\theta$ axis when $\tan \theta_c / \tan \theta_M = 1$, see Fig. 4 in *M85a*. In the antiparallel region, it rotates clockwise with increase in $|\theta_c|$ with no special conditions arising. The dependence on θ_c of the wavelength-dispersion component, $|\Delta\omega_\lambda|$, is shown *versus* the dimensionless variable $t = \tan \theta_c / \tan \theta_M$ in Fig. 2(b) for two values of $|\Delta\theta_M|$, the intercept on the $\Delta\omega$ axis.† Note that the difference between the non-monochromator case (Fig. 2a) and the monochromator case (Fig. 2b) is that the point of inversion is displaced from $\theta_c = 0^\circ$ to $\theta_c = \theta_M$.

Wavelength-dispersion component in *R93*

The wavelength-dispersion component in *R93* is recorded in Fig. 5 as the dependence of $|\Delta\omega_\lambda|$ (given as FWHM) on θ_c calculated for a series of wavelengths from 0.3 to 2.2 Å. All curves make a zero intercept on the $|\Delta\omega_\lambda|$ axis at $\theta_c = 0^\circ$. This is despite the statement in the figure caption that δ_{cryst} (which is effectively $|\Delta\theta_M|$, see Fig. 4 in *R93*) is a measurable non-zero quantity [see equations (6a) and (7a)]. The data in Fig. 5 in *R93* correspond therefore to the dependence depicted by the dashed line in Fig. 2(b).

From the data for FWHM given in Fig. 5 in *R93*, one may deduce, for $\lambda = 0.3$ Å, that, at $\theta_c = 45^\circ$, $\Delta\lambda/\lambda$ is equivalent to 0.035° . Therefore, for $\theta_M = \theta_c = 2.74^\circ$, $(\Delta\lambda/\lambda) \tan \theta_M = (\Delta\lambda/\lambda) \tan \theta_c = 0.0017^\circ = \Delta\theta_M$ (FWHM). If $f = 0.75$ (Table 2a in *R93*), then the base width (Fig. 3 in *R93*) is 0.0022° . Using these values, one can indicate in Fig. 2(b) how the two values of $|\Delta\omega_\lambda|$ vary with t , *i.e.* $|\Delta\omega_\lambda| \propto |t - 1|$.

$|\Delta\theta_M|$ constitutes a constant factor which displaces the whole curve in the antiparallel region; compare the dashed line

* A referee has suggested that it might be useful to address the question 'Are the two aspects of the inner morphology of the crystal, namely the size and orientation of the crystallites, separable by diffraction techniques, including analysis of the wavelength dependence?'. As Wilson (1949) observes (p. 4, equation 3), the crystallite-size effect, ε , has a $\lambda/\cos \theta$ dependence. By contrast, the orientation effect, η , if isotropic, has neither λ nor θ dependence in angle space. Realistic estimates of the individual components should, therefore, be capable of extraction, particularly in $\Delta\omega, \Delta 2\theta$ space, from analysis of experimental data over a range of θ at one wavelength or investigation at different wavelengths (the latter readily attainable with synchrotron radiation). This does not, of course, modify the fact that, in any given observation of reflection shapes, the two components are effectively combined by convolution.

† The sign allotted to t depends on the convention chosen, see Mathieson & Stevenson, 1993.

with the lower full line in Fig. 2(b). It may be pointed out that the intercept at $\theta_c = 0^\circ$, i.e. $t = 0$, can only be zero if $(\Delta\lambda/\lambda) = 0$, which contradicts the basis of the model in Fig. 4 of R93. Recognition and estimation of this component, $|\Delta\theta_M|$, is therefore advisable as a fundamental step in establishing the wavelength-dispersion component for (a) determining the scan range and (b) the modelling of one-dimensional profiles of Bragg reflections when one is aiming at careful single-crystal synchrotron-radiation studies.

In respect of the non-zero status of $|\Delta\omega_\lambda|$ at $\theta_c = 0^\circ$, reference may be made to Willis (1960), which deals with a somewhat similar situation involving an extended-face crystal rather than a small specimen crystal (see also Mathieson, 1988).

6. Mosaic distribution

Nearly 20 years ago, Boehm, Prager & Barnea (1974) demonstrated experimentally with Si that the structure (inner morphology) of a ground spherical single crystal corresponded to a 'perfect' core and an 'imperfect' outer skin. Subsequently, Le Page & Gabe (1978) used this model to refine structural parameters from ground spherical crystals. This approach was tested in respect of three crystals. Application of this approach requires, in principle, at least three parameters, two to describe the mosaic distributions and a weight factor for the relative amounts of the two components.

In R93, a simpler approach is taken in that only one parameter, η , is allowed to represent an average mosaic distribution and that is derived [equation (13) in R93] by averaging the fit of measured FWHM with FWHM calculated according to equations (6a), (6b) and (6c) in R93. If the application of equations (6a), (6b) and (6c) is not strictly valid, see §§3 and 4 above, then further steps based on these equations become questionable.

It would be more direct to establish mosaic-distribution estimates from experimental measures rather than mathematical operations involving a number of probably interacting parameters. As is indicated by Fig. 1(a), direct estimate in $\Delta\omega, \Delta 2\theta$ space of even a limited number of reflections could yield useful information on the distribution of $\mu (= \eta)$. See, for example, the fragment distribution shown in Mathieson (1982)

and the anisotropic distributions in Mathieson & Stevenson (1986).

In the concluding remarks in R93, Rossmannith points to 'varying - and therefore unknown - mosaic structure' and links this with the 'difficulty of obtaining integrated intensities with sufficient accuracy using synchrotron radiation...'. There is no reason to imply that this information concerning mosaic structure is difficult to achieve. It is possible, if time-consuming, to establish reasonably detailed information on mosaic distributions using $\Delta\omega, \Delta 2\theta$ techniques (see references above).

I am most grateful to my colleagues Drs A. W. Stevenson and S. W. Wilkins for their patience in discussions and for valuable comments on the text as it developed. I am also grateful to an anonymous referee for the suggestion to clarify §4 further. The author is, however, solely responsible for statements made in this communication.

References

- ALEXANDER, K. E. & SMITH, G. S. (1962). *Acta Cryst.* **15**, 983-1004.
 ARNDT, U. W. & WILLIS, B. T. M. (1966). *Single Crystal Diffractometry*. Cambridge Univ. Press.
 BOEHM, J. M., PRAGER, P. R. & BARNEA, Z. (1974). *Acta Cryst.* **A30**, 335-337.
 DESTRO, R. & MARSH, R. E. (1993). *Acta Cryst.* **A49**, 183-190.
International Tables for Crystallography (1992). Vol. C, p. 37. Dordrecht: Kluwer Academic Publishers.
 LE PAGE, Y. & GABE, E. J. (1978). *J. Appl. Cryst.* **11**, 254-256.
 MATHIESON, A. MCL. (1982). *Acta Cryst.* **A38**, 378-387.
 MATHIESON, A. MCL. (1984). *Acta Cryst.* **A40**, 355-363.
 MATHIESON, A. MCL. (1985a). *Acta Cryst.* **A41**, 309-316.
 MATHIESON, A. MCL. (1985b). *Acta Cryst.* **A41**, 603-605.
 MATHIESON, A. MCL. (1988). *Acta Cryst.* **A44**, 239-243.
 MATHIESON, A. MCL. & STEVENSON, A. W. (1986). *Acta Cryst.* **A42**, 223-230.
 MATHIESON, A. MCL. & STEVENSON, A. W. (1993). *Acta Cryst.* **A49**, 655-661.
 ROSSMANITH, E. (1992). *Acta Cryst.* **A48**, 596-610.
 ROSSMANITH, E. (1993). *Acta Cryst.* **A49**, 80-91.
 STOKES, A. R. (1948). *Proc. Phys. Soc. London Sect. A*, **61**, 382-391.
 WILLIS, B. T. M. (1960). *Acta Cryst.* **13**, 763-766.
 WILSON, A. J. C. (1949). *X-ray Optics*. London: Methuen.

International Union of Crystallography

Acta Cryst. (1994). **A50**, 126

Restructuring of the IUCr editorial office

Following the promotion of Mr Michael Dacombe from Technical Editor to Executive Secretary, it was considered an opportune time to restructure the editorial office to reflect better the greater variety of work now carried out and to clarify the responsibilities of the staff.

Mr Peter Strickland has been appointed as Managing Editor with overall responsibility for both the technical editing and the centralized checking. Mrs Sue King has been appointed as Technical Editor. Dr Amanda Berry has been appointed as Assistant Technical Editor with special responsibility for the centralized checking. There are three Senior Editorial Assistants and six Editorial Assistants. Mr Brian McMahon is the Research and Development Officer and his assistant is Dr M. Hoyland. The total number of graduate staff in the editorial office is 14.